مجله بلورشناسی و کانی شناسی ایران
شمارهٔ ۲، پاییز و زمستان۸۶، از صفحهٔ ۴۹۳ تا ۵۱۴
انجمن بلورشناسی و کانی شناسی ایران

دگرگونی مجاورتی در هستهٔ دگرگون شاهیندژ (SMC) – شمالغرب ایران؛ تعیین دما و فشار و شواهد بافتی برای پدیدهٔ ذوب بخشی در متاپلیتها

منیر مجرد، محسن مؤذن، محسن مؤید

۱- دانشگاه تبریز، دانشکده علوم طبیعی، گروه زمین شناسی
پست الکترونیکی: mmodjarrad@yahoo.com

(دریافت مقاله ۱۳۸۵/۱۰/۱۷ ، دریافت نسخه نهایی ۱۳۸۶/۴/۲)

چکیده: سنگهای رسی دگرگون شده شرق شاهیندژ (SMC) با نفوذ گرانیتوئید پیچاقچی طی فاز کوهزائی لارامید، به صورت مجاورتی دگرگون شده‌اند. پاراژنز غالب در سنگهای رسی دگرگون شده شامل کوارتز+پلاژیوکلاز+بیوتیت+کردیریت±کلریت±آلکالی فلدسپات± مسکویت± آندالوزیت± سیلیمانیت و ± گارنت است. دما و فشار در هالهٔ مجاورتی SMC برای مجموعه حاوی آندالوزیت+کردیریت که فراوان‌ترین مجموعه کانیایی در هالهٔ مجاورتی است، با استفاده از برنامهٔ THERMOCALC حدود ۳/۵ کیلوبار و ۵۰۰ °C ± ۵۰ °C محاسبه شده است. بعلاوه محل دقیق واکنش شکست مسکویت+بیوتیت در نمودار دما- فشار ۶۵۰ °C ±۴۰ °C در فشار یاد شده برآورد شده است. موقعیت دمایی محاسبه شده همخوانی خوبی با داده‌های تجربی موجود در منابع سنگ‌شناسی دگرگونی دارد. سنگ‌های رسی دگرگون شده در بخش شمال-شرقی SMC حاوی پاراژنز دمای بالای کوارتز+بیوتیت+گارنت+سیلیمانیت+ پلاژیوکلاز± کردیریت±آلکالی فلدسپات هستند. با توجه به مجموعهٔ کانیایی و بافتهای میکروسکوپی مشاهده شده، سنگهای هالهٔ مجاورتی در فشار حدود ۴ کیلوبار و دمایی معادل ۷۵۰ °C< ذوب‌بخشی را تجربه کرده‌اند. در سنگهایی که به صورت بخشی ذوب شده‌اند، پروفیروبلاستهای گارنت همراه با کوارتز دانه درشت دیده می‌شوند. کردیریت هم به صورت حاشیه‌هایی از گارنتهای قدیمی و هم در زمینه در طی دگرگونی ناحیه‌ای تشکیل شده است تمام کردیریتها به پینیت دگرسان شده‌اند. ادخالهایی از فیبرولیت در زمینه سنگ به فراوانی وجود دارد.

واژه‌های کلیدی: *متاپلیت، THERMOCALC، شکست مسکویت+بیوتیت، شواهد بافتی، ذوب بخشی، هسته دگرگونی شاهیندژ (SMC)، ایران.*

IRANIAN SOCIETY of CRYSTALLOGRAPHY and MINERALOGY

No. 2, 1386/2007 Fall & Winter

IRANIAN JOURNAL of CRYSTALLOGRAPHY and MINERALOGY

Contact metamorphism in the Shahindezh Metamorphic Core (SMC)-NW Iran; PT conditions and microstructural evidence for partial melting of metapelites

M. Modjarrad, M. Moazzen, M. Moayyed

1- Faculty of Natural Sciences, Department of Geology, University of Tabriz, Iran
E-mail: mmodjarrad@yahoo.com

(Received:7/1/2007, received in revised form:24/6/2007)

Abstract: Contact metamorphism in the Shahindezh Metamorphic Core (SMC), which is occurred due to intrusion of Pichaghchi granodiorite during Laramian orogeny (Upper Cretaceous), is studied here. The well developed mineral parageneses at the aureole is quatz + plagioclase + biotite + cordierite ± chlorite ± K-feldspar ± muscovite ± andalusite ± sillimanite ± garnet. Pressure and temperature of the contact metamorphism at the SMC for andalusite + cordierite –bearing assemblages (the most common paragenesis at the aureole) are estimated ~3.5 ± 1.5 kbar and 500 ± 50 °C using THERMOCALC computer program. Also the exact position of the muscovite + biotite breakdown reaction at the PT space, is calculated. Temperature for muscovite-biotite breakdown was about 650 ± 40 °C at 3.5 kbar. The calculated position of the reaction curve, is in good agreement with published experimental data. The metapelites at the north-eastern part of the SMC contain high-temperature assemblage quartz + biotite + garnet + sillimanite + plagioclase ± cordierite ± K-feldspar. The mineral assemblages and reaction textures in the aureole rocks record temperature about <750 °C at the sillimanite -cordierite zone and pressure ~ 4 kbar, determined using petrogenetic grids. In the partially molten rocks garnet porphyroblasts are associated with coarse-grained quartz. Cordierites occurred both at the rims of residual garnets crystallized during regional metamorphism and in the matrix. All cordierites are altered to pennite. Fibrolite inclusions in the matrix cordierites are common.

Keywords: *Metapelites; THERMOCALC; Muscovite-biotite breakdown; Microstructure; Partial melting; Shahindezh Metamorphic Core; Iran*

1. Introduction

The best tools to estimate pressure (P) and temperature (T) of metamorphism in thermal aureoles is stability of aluminosilicates and mineral chemistry of ferromagnesian minerals. Using thermodynamic data for each mineral such as enthalpy, entropy, molar volume and heat capacity at the standard conditions [1], and by using the thermodynamic master equation based on Gibbs free energy, it is possible to calculate the exact position of mineral reaction curves on a PT diagram. Pressure is usually constant during contact metamorphism, therefore crystallization temperature of a new phase can be calculated at constant pressure.

The process of dehydration melting in which water is transferred from hydrous minerals to melt, without direct participation of an aqueous fluid phase, is a potentially important agent for dehydration of high-grade terrains [2]. Prograde metamorphism is a dehydration process, so water generated by the reactions can controls solidus and melting reactions rates [3]. The hypothesis is that water is in excess during the prograde metamorphic path. It can leave the system by melt extraction in dehydrating rocks [4].

Dehydration melting reactions for typical crustal lithologies have a positive slope in P-T diagram. Therefore partial melting may occur either by an increase in temperature or decrease in pressure [5-8].

However, the degree of melt extraction, the fate of dissolved water and the possibilities for retrograde reaction have been much debated. Some of the questions raised, can be illuminated by studies of the prograde microstructures of partially melted rocks.

Recently, prograde and retrograde microstructures that are common in low-pressure migmatitic rocks have been well documented (e.g. in the Proterozoic Namaqualand Metamorphic Complex, South Africa [9]; Shuswape metamorphic core complex, Canadian Cordillera [6] and Pointe Geologie migmatitic complex [3]).

In east of Shahindezh and west of Takab in western Iran, a variety of igneous, sedimentary and metamorphic rocks are exposed. Young granite and granodiorite, older alkali granite and gabbro are igneous rocks of the area. Old pelitic sedimentary rocks (Precambrian) are metamorphosed to porphyroblast-bearing metamorphic rocks during Catangaian orogeny [10, 11]. These rocks have experienced several phases of regional poly-metamorphism and a final contact metamorphism. This contribution concentrates on nature of contact metamorphism, while regional metamorphism and deformation will be discussed in another paper. Apart from the geological map of the Shahindezh area [12] there is no published account on mechanism of metamorphism in this area.

We try to estimate PT condition of contact metamorphism here, using textural relations, mineral composition and thermodynamic data. Also the

temperature of breakdown of muscovite and biotite in the contact aureole of SMC will be discussed. At the east of the SMC, well known microstructures confirming partial melting of metapelites, are observed. Also, the probable melting reactions and maximum temperature of partial melting at the SMC aureole, using petrogenetic grid, are addressed.

2. Geological setting

Shahindezh area is located in the central Iran geological zone [13, 14] and is bounded with Sanadaj-Sirjan zone in the south and Sahand-Bazman zone in the east. The pelitic rocks of the area are probably equivalent to the old rocks of the central Iran which are metamorphosed up to amphibolite facies (Chapdony formation, [15 - 18]). The fossil-bearing Palaeozoic rocks of the area, covering the metapelites, are not metamorphosed. Therefore a Precambrian age for regional metamorphism is likely. Sediments of Kahar Formation, fossil-bearing dolomites of Soltanieh Formation and micaceous sandstones of Lalun Formation cover the metapelites continuously. Apart from Kahar Formation which shows very low grade metamorphism, the other rocks are not metamorphosed. Granitoid rocks have vast outcrops around Pichaghchi, Mahmoudabad and Khazaiibala villages (Fig. 1). There are numerous small outcrops of granitoid rocks which are very similar to the main granitoid bodies in terms of mineralogy and field relations. Age determination based on K-Ar method on Pichaghchi granitoid gives an Upper Cretaceous age [19].

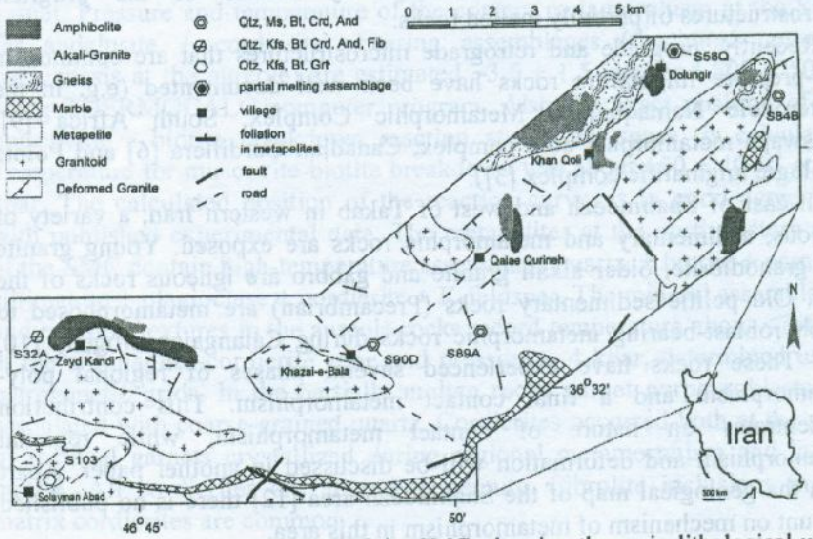

Fig. 1 Simplified geological map of the SMC, showing the main lithological units, modified after Geological Map of Shahindezh [12]. Representative mineral assemblages in the metapelites are shown.

The intrusion of this granitoid has caused contact metamorphism overprinted the older regional metamorphism (Fig. 1). It seems that intrusion of this pluton has been contemporaneous to or after closure of Neo-Thetys ocean due to Laramid Orogeny. A part of the granitoid rocks in the eastern part of the area show deformational patterns due to intrusion contemporaneous to orogeny. Cretaceous limestones show recrystallisation in contact with pluton. This shows intrusion of the granitoid after deposition of Cretaceous limestones.

3. Petrography

3. 1.Granitoid pluton

These rocks occupy vast parts of the studied area. The main outcrop is around Pichaghchi and Gharehzagh villages. In fact the northern part of the study area is made from these rocks. Also outcrops in the central part of the area around Dolungir, Qalae Qurineh, south and west of Khazai-e-Bala and Zeyd kandi can be found (Fig. 1). Limited outcrops are seen along the main Shahindezh-Takab road near Mahmoudabad village. These rocks can be divided into two main groups, amphibole-bearing rocks and amphibole-free pegmatites. The most rocks of the first group contain quartz, plagioclase, K-feldspar, amphibole, biotite and titanite. The rocks are pale grey in hand specimen with relatively large mafic minerals. These rocks have 10-35 modal% mafic minerals, mainly amphibole (5-25 modal%) and biotite (3-<10 modal%). Accessory phases such as apatite, zircon and oxide minerals are present. Sericite and chlorite are alteration products. Usually the modal percentage of plagioclase is higher than that of K-feldspar. Plagioclase shows alteration in some samples but it shows idiomorphic crystals with optical zoning in most of the samples. Myrmekite texture is developed either at the margins of K-feldspar and plagioclase or at boundary between quartz and K-feldspar. K-feldspar and plagioclase reach up to 5 mm in size while amphiboles are up to 2.5 mm in size. They are prismatic idiomophic and pale to dark green in colour.

There are some mafic enclaves within the granitoids (maximum 80 cm in length). Biotite is higher than amphibole in these enclaves. These enclaves are abundant and show an approximate N40E orientation.

The second group of granitoids lack amphibole and appear as pegmatites. The mafic minerals in these rocks are biotite and chlorite after biotite. There is no white mica in the studied samples of granitoids.

3. 2. Metapelites

Metapelites contain porphyroblasts of cordierite, andalusite, garnet and fibrolite in a finer groundmass of quartz, biotite, muscovite, K-feldspar, plagioclase (albite) and chlorite (Fig 2). Cordierite porphyroblasts (with a diameter of ca. 0.5cm) are visible in the hand specimens. Oxides, tourmaline,

apatite, zircon and graphite are minor phases in these rocks. Cordierite is the main contact metamorphic mineral crystallized in the rocks. Contact metamorphic garnet is not very common in the studied samples and occurs as 0.2 mm sized crystals, only in samples from the vicinity of Soliemanabad village (SW of the area). Sillimanite is fibrolitic in most of the samples. Prismatic sillimanite was found in a few samples.

The main mineral parageneses in the rocks are:

Qtz + Pl + Bt ± Kfs ± Ms + Crd ± And ± Sil [p1]

Qtz + Pl + Bt ± Kfs + Grt ± Fib [p2]

Partially melted rocks appear at the north-eastern part of the area. There will be discussed in more details later. Chlorite and muscovite are crystallized during contact metamorphism and cross-cut the former foliation. The high number of chlorite and muscovite shows high degree of overstepping due to intrusion of the pluton. There are some fibrolite in the hornfelses as a common feature, which are retrograde metamorphic products after biotite [20].

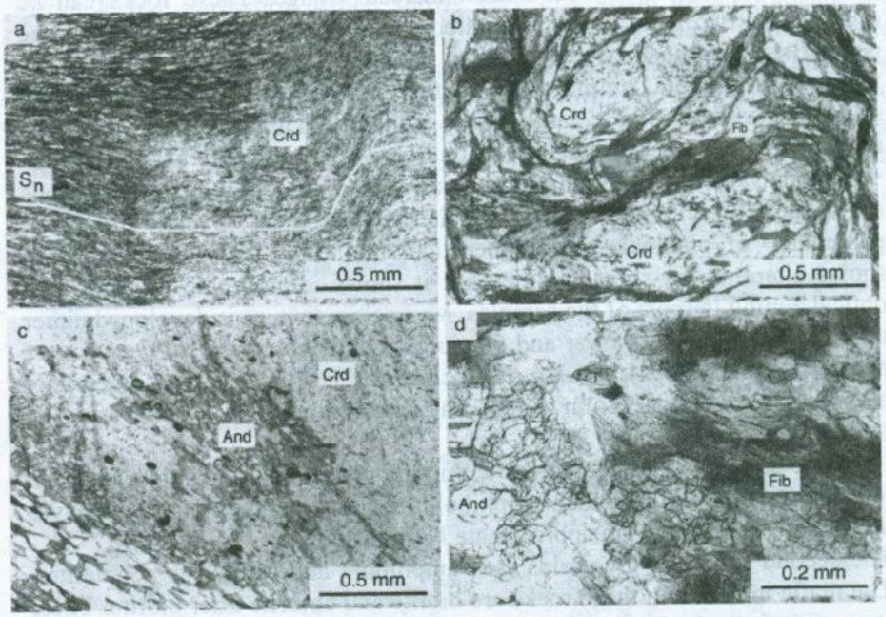

Fig. 2 a) Microphotographs showing post-deformational growth of cordierite during contact metamorphism (PPL). Trend of inclusions in the cordierite is continuing of the latest matrix foliation (S n), formed during regional metamorphism. b) cordierite in hornfelsic metapelites. In this sample rock foliation is obscured due to contact metamorphism. Small amounts of fine grained fibrolite are grown after biotite. c) Andalusite within cordierite porphyroblast from metapelites. d) Andalusite partly replaced by fibrolite.

4. Mineral Chemistry

Minerals in representative samples of contact metamorphic rocks of the SMC were analysed. A Cameca SX100 electron microprope in the GeoForschungsZentrum (GFZ) in Potsdam, Germany was used under standard condition (15 kV, 10-20 nA, PAP correction procedure) for analyses. Natural and synthetic standard minerals (Fe_2O_3 [Fe], rhodonite [Mn], rutile [Ti], MgO [Mg], wollastonite [Si, Ca], fluorite [F], orthoclase [Al, K] and albite [Na]) were used for calibration. The analytical spot diameter was set between 3 and 5 μm, keeping the same current conditions. Formula of biotite was calculated on the basis of 22 oxygens, cordierite on the basis of 18 oxygens and feldspar on the basis of 8 oxygens. Fe^{3+}/Fe^{2+} ratio was calculated using stoichiometry and activity of end members were calculated by AX computer program (ftp://www.esc.cam.ac.uk /pub/minps/AX). The activity of cordierite end members were calculated on the anhydrous basis with R_{mex}=0.2 and Margules interaction parameters of W_{FeMg}=1.5 and W_{MgMn}=1.5 (KJ). For feldspar activities the model of Holland and Powell (1992) and for biotite ordered non-ideal mixing in two sites model was used. The total of cations in octahedral and tetrahedral sites of biotites was about 6.9 for 11 oxygens. R_{max} of 0.15 was considered for biotite. The mineral names abbreviations are from Kretz [21].

4. 1. Biotite

Analyses of biotite are provided in Table 1. The X_{Mg} in the analysed biotites is 0.45-0.56 clustering around 0.52. Al^{IV} content is 1.083-1.387 and Al^{VI} content is 0.38-0.66. TiO_2 varies from 1.21 to 1.68. Figure 3 illustrates the analysed biotites in Al^{IV} versus X_{Mg} diagram. There is a positive relation between thes two factors. This is more clear from Fig. 4a which is compatible with reverse relation between X_{Mg} and SiO_2 in the biotites (Table 1).

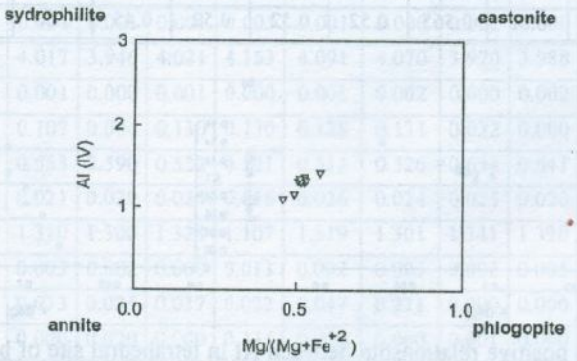

Fig. 3 Compositional variability of biotite due to the Tschermak (Al in tetrahedral site) and Fe-Mg substitutions.

Table 1 Representative microprobe analyses of biotite.

	Biotite									
SiO_2	36.10	35.57	35.23	36.11	35.75	36.38	39.38	35.29	36.29	38.12
TiO_2	1.59	1.68	1.46	1.60	1.40	1.47	1.21	1.50	1.62	1.54
Al_2O_3	20.07	20.55	20.20	20.51	20.03	20.07	18.69	19.42	19.94	20.38
Cr_2O_3	0.00	0.03	0.05	0.03	0.04	0.05	0.05	0.02	0.03	0.03
Fe_2O_3	0.84	0.17	3.10	0.00	0.00	0.00	0.00	0.00	0.68	0.00
FeO	17.56	17.39	15.83	17.61	17.63	17.68	18.86	18.23	18.12	16.00
MnO	0.07	0.05	0.13	0.07	0.08	0.12	0.05	0.06	0.09	0.09
MgO	10.78	10.68	11.53	10.68	10.62	10.54	8.80	10.10	10.58	8.69
CaO	0.00	0.00	0.00	0.03	0.00	0.04	0.48	0.07	0.02	0.09
Na_2O	0.23	0.10	0.79	0.45	0.22	0.12	1.13	0.17	0.12	0.72
K_2O	8.21	8.43	7.90	8.28	8.50	8.27	6.71	8.14	8.35	7.49
Total	95.45	94.66	96.23	95.38	94.28	94.75	95.37	93.01	95.85	93.16
Cations per 22 (O)										
Si	2.696	2.676	2.613	2.695	2.705	2.731	2.917	2.715	2.706	2.860
Ti	0.089	0.095	0.081	0.090	0.080	0.083	0.067	0.087	0.091	0.087
Al	1.767	1.823	1.767	1.805	1.787	1.776	1.632	1.761	1.753	1.803
Cr	0.000	0.002	0.003	0.002	0.002	0.003	0.003	0.001	0.002	0.002
Fe^{3+}	0.047	0.009	0.173	0.000	0.000	0.000	0.000	0.000	0.038	0.000
Fe^{2+}	1.096	1.094	0.982	1.099	1.116	1.110	1.168	1.173	1.130	1.004
Mn	0.004	0.003	0.008	0.004	0.005	0.008	0.003	0.004	0.006	0.006
Mg	1.200	1.197	1.275	1.188	1.198	1.179	0.971	1.158	1.176	0.972
Ca	0.000	0.000	0.000	0.002	0.000	0.003	0.038	0.006	0.002	0.007
Na	0.033	0.015	0.114	0.065	0.032	0.017	0.162	0.025	0.017	0.105
K	0.783	0.810	0.748	0.789	0.821	0.793	0.635	0.800	0.795	0.718
Al^{IV}	1.304	1.324	1.387	1.305	1.295	1.269	1.083	1.285	1.294	1.14
Al^{VI}	0.463	0.499	0.38	0.50	0.492	0.507	0.549	0.476	0.459	0.663
X_{Mg}	0.52	0.52	0.565	0.52	0.52	0.52	0.45	0.50	0.51	0.49

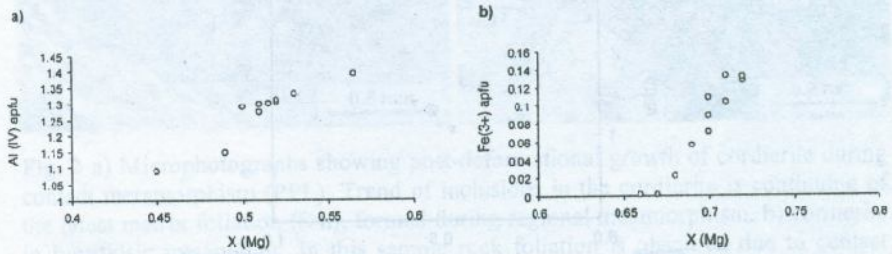

Fig. 4. a) The positive relationship between Al in tetrahedral site of biotite and X_{Mg} in the analysed biotite from sample S90D. b) Increasing of X_{Mg} in cordierite by increasing of Fe^{3+}.

4. 2. Cordierite

The chemical composition of contact metamorphic cordierites in the Shahindezh samples is similar with 66-72% Mg-cordierite and 1-1.5% Mn-cordierite (Table 2). The Fe^{2+} content is 0.511-0.641 atoms per formula unit on the basis of 18 oxygens. There is a negative relation between Mg number and SiO_2 in the studied cordierites (similar to biotite) and a positive relation between X_{Mg} and Fe^{3+} content (Fig. 4b).

4. 3. Plagioclase

The analysed plagioclase are made of 91-95% albite and 5-9.5% anorthite end members with a composition close to oligoclase (Table 3).

Table 2 Representative microprobe analyses of cordierite.

	Cordierite										
SiO_2	48.88	48.80	49.27	48.61	48.46	48.54	48.68	48.77	49.10	48.70	49.30
TiO_2	0.01	0.01	0.01	0.01	0.04	0.01	0.00	0.02	0.00	0.00	0.02
Al_2O_3	33.55	33.57	32.81	33.55	34.72	34.47	34.54	32.83	33.12	33.24	33.72
Cr_2O_3	0.00	0.01	0.00	0.01	0.00	0.01	0.03	0.00	0.02	0.00	0.00
Fe_2O_3	0.89	1.40	0.71	1.70	1.71	1.69	1.75	0.28	0.00	1.13	1.34
FeO	6.61	6.52	6.91	6.14	6.14	6.07	6.29	7.39	7.50	6.63	6.45
MnO	0.29	0.24	0.33	0.28	0.19	0.31	0.28	0.029	0.23	0.27	0.29
MgO	8.74	8.66	8.55	8.74	7.32	8.79	8.73	8.77	8.67	8.80	8.67
CaO	0.01	0.03	0.02	0.00	0.12	0.02	0.01	0.02	0.05	0.01	0.04
Na_2O	0.14	0.17	0.17	0.19	0.11	0.24	1.14	0.00	0.00	0.10	0.19
K_2O	0.01	0.00	0.15	0.00	1.04	0.20	0.00	0.01	0.00	0.00	0.08
Total	99.13	99.41	98.93	99.23	99.85	100.35	101.45	98.38	98.69	98.88	100.10
Cations per 18 (O)											
Si	4.969	4.953	5.026	4.941	4.917	4.887	4.866	5.003	5.015	4.968	4.968
Ti	0.001	0.001	0.001	0.001	0.003	0.001	0.000	0.002	0.000	0.000	0.002
Al	4.021	4.017	3.946	4.021	4.153	4.091	4.070	3.970	3.988	3.997	4.006
Cr	0.000	0.001	0.000	0.001	0.000	0.001	0.002	0.000	0.002	0.000	0.000
Fe^{3+}	0.068	0.107	0.054	0.130	0.130	0.128	0.131	0.022	0.000	0.087	0.102
Fe^{2+}	0.562	0.553	0.590	0.522	0.521	0.511	0.526	0.634	0.641	0.566	0.544
Mn	0.025	0.021	0.029	0.024	0.016	0.026	0.024	0.025	0.020	0.023	0.025
Mg	1.324	1.310	1.300	1.324	1.107	1.319	1.301	1.341	1.320	1.338	1.302
Ca	0.001	0.003	0.002	0.000	0.013	0.002	0.001	0.002	0.005	0.001	0.004
Na	0.028	0.033	0.034	0.037	0.022	0.047	0.221	0.000	0.000	0.020	0.037
K	0.001	0.000	0.020	0.000	0.135	0.026	0.000	0.001	0.000	0.000	0.010
MgCrd	0.70	0.70	0.69	0.72	0.68	0.72	0.71	0.68	0.67	0.70	0.71
MnCrd	0.013	0.011	0.015	0.013	0.01	0.014	0.013	0.013	0.01	0.012	0.013

Table 3 Representative microprobe analyses of plagioclase.

	Plagioclase						
SiO_2	71.71	66.23	66.40	67.70	66.55	65.99	67.24
TiO_2	0.00	0.00	0.00	0.03	0.00	0.01	0.01
Al2O3	18.87	22.38	22.15	21.13	21.34	21.37	21.54
Cr2O3	0.00	0.00	0.00	0.00	0.00	0.00	0.00
Fe2O3	0.31	0.17	0.24	0.23	0.30	0.20	0.17
FeO	0.00	0.00	0.00	0.00	0.00	0.00	0.00
MnO	0.00	0.03	0.00	0.02	0.00	0.01	0.00
MgO	0.00	0.02	0.00	0.00	0.00	0.00	0.00
CaO	1.38	1.90	2.04	1.30	1.48	1.47	1.55
Na2O	8.63	10.86	10.82	11.38	10.94	10.85	11.29
K2O	0.14	0.06	0.07	0.07	0.09	0.08	0.06
Total	101.04	101.65	101.72	101.86	100.70	99.98	101.86
	Cations per 8 (O)						
Si	3.067	2.866	2.872	2.919	2.903	2.898	2.901
Ti	0.000	0.000	0.000	0.001	0.000	0.000	0.000
Al	0.951	1.142	1.129	1.074	1.097	1.106	1.096
Cr	0.000	0.000	0.000	0.000	0.000	0.000	0.000
Fe3+	0.010	0.005	0.008	0.008	0.010	0.007	0.005
Fe2+	0.000	0.000	0.000	0.000	0.000	0.000	0.000
Mn	0.000	0.001	0.000	0.001	0.000	0.000	0.000
Mg	0.000	0.001	0.000	0.000	0.000	0.000	0.000
Ca	0.063	0.088	0.095	0.060	0.069	0.069	0.072
Na	0.716	0.911	0.907	0.951	0.925	0.924	0.945
K	0.008	0.003	0.004	0.004	0.005	0.004	0.003
XAn	0.08	0.09	0.095	0.06	0.07	0.07	0.07
XAb	0.92	0.91	0.91	0.94	0.93	0.93	0.93

5. Metamorphic reactions

Since the width of the contact aureole is not considerable, it is not possible to separate the mineralogical zones on map. In spite of this problem, it is possible to conclude the metamorphic reactions using an upgrade (i.e. toward the igneous contact) collection of pelitic samples. The appearance of chlorite, muscovite and fibrolite has a widespread, whereas the appearance of cordierite, garnet, K-feldspar and sillimanite porphyroblasts all occur in the biotite zone of the former regional metamorphism. Compatibility diagrams (AFM diagrams) are constructed to infer the contact metamorphic

reactions (Fig. 5). Fine grain garnets in the hornfelses are formed by the following reaction:

$$Chl + Qtz = Grt + Bt + H_2O \qquad [r1]$$

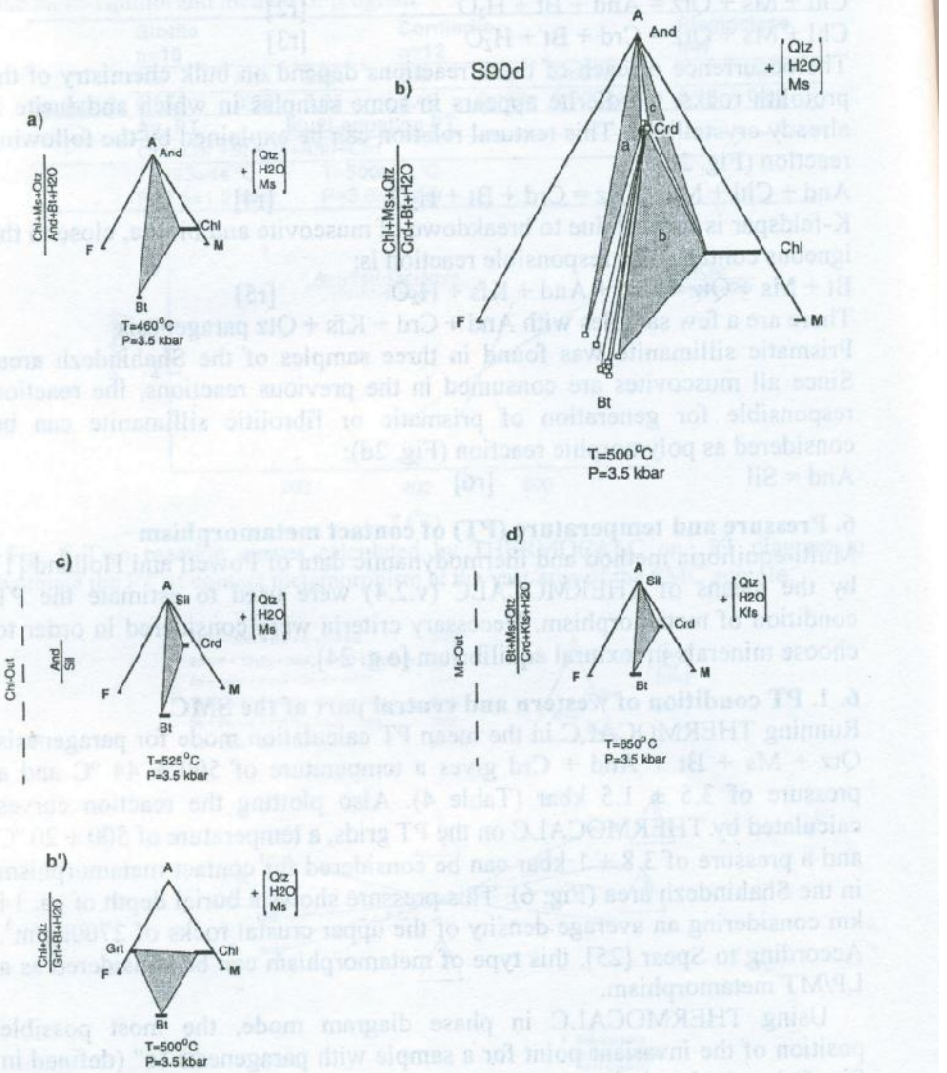

Fig. 5 Compatibility diagrams (KFMASH system) for mineral assemblages of the SMC aureole. All diagrams are plotted schematically, except for diagram 5b, which is plotted using real mineral compositions. Probable responsible reactions and estimation of PT of stability of parageneses, using petrogenetic grid after [22] are shown.

These hornfelses contain either andalusite or cordierite (Fig. 2b) or both [e.g. 23]. Individual occurrences of these two minerals in the studied rocks show the operation of the following reactions:

$Chl + Ms + Qtz = And + Bt + H_2O$ [r2]

$Chl + Ms + Qtz = Crd + Bt + H_2O$ [r3]

The occurrence of each of these reactions depend on bulk chemistry of the protolith rocks. Cordierite appears in some samples in which andalusite is already crystallized. This textural relation can be explained by the following reaction (Fig. 2c):

$And + Chl + Ms + Qtz = Crd + Bt + H_2O$ [r4]

K-feldspar is formed due to breakdown of muscovite and biotite, close to the igneous contact. The responsible reaction is:

$Bt + Ms + Qtz = Crd + And + Kfs + H_2O$ [r5]

There are a few samples with And + Crd + Kfs + Qtz paragenesis.

Prismatic sillimanite was found in three samples of the Shahindezh area. Since all muscovites are consumed in the previous reactions, the reaction responsible for generation of prismatic or fibrolitic sillimanite can be considered as polymorphic reaction (Fig. 2d):

$And = Sil$ [r6]

6. Pressure and temperature (PT) of contact metamorphism

Multi-equilibria method and thermodynamic data of Powell and Holland [1] by the means of THERMOCALC (v.2.4) were used to estimate the PT condition of metamorphism. Necessary criteria were considered in order to choose minerals in textural equilibrium [e.g. 24].

6. 1. PT condition of western and central part of the SMC

Running THERMOCALC in the mean PT calculation mode for paragenesis Qtz + Ms + Bt + And + Crd gives a temperature of 500 ± 44 °C and a pressure of 3.5 ± 1.5 kbar (Table 4). Also plotting the reaction curves calculated by THERMOCALC on the PT grids, a temperature of 500 ± 20 °C and a pressure of 3.8 ± 1 kbar can be considered for contact metamorphism in the Shahindezh area (Fig. 6). This pressure shows a burial depth of ca. 14 km considering an average density of the upper crustal rocks of 2700kg/m^3. According to Spear [25], this type of metamorphism can be considered as a LP/MT metamorphism.

Using THERMOCALC in phase diagram mode, the most possible position of the invariant point for a sample with paragenesis "c" (defined in Fig. 5) is calculated. Considering the low standard deviations in P and T, this point can be considered as invariant point for the multiple equilibria reactions discussed above (Fig. 7).

Table 4 Average end-member activities in the sample S90D which is used as THERMOCALC inputs. Activity of quartz, muscovite, chlorite, andalusite and H_2O is supposed to be 1.Pressure and temperature are calculated both by average mode and multi-equilibrium method of program.

	Biotite n=10			Cordierite n=12			Plagioclase n=7	
	Phl	Ann	East	Crd	fCrd	MnCrd	An	Ab
Av. activity	0.053	0.03	0.05	0.49	0.113	0.00021	0.12	0.93
	Av. PT		Multi-equation PT					
	Qtz+Chl +Bt+Ms+And+Crd							
	T=493±44 °C		T=500±20 °C					
	P=3.5±1.5 kbar		P=3.8±1 kbar					

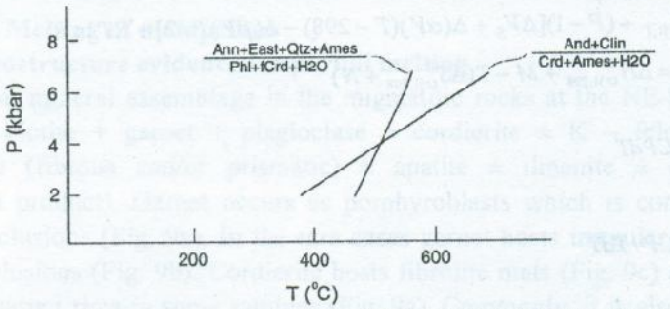

Fig. 6 Two reaction curves calculated by THERMOCALC on PT diagram to estimate the PT of contact metamorphism at the vast area of the SMC aureole.

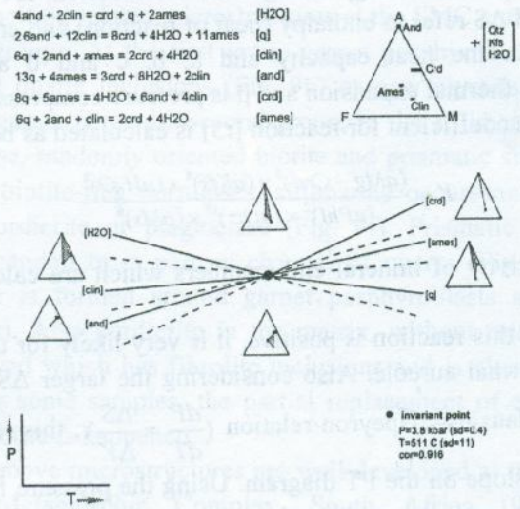

Fig. 7 Possible position of the invariant point for the parageneses c (Fig. 6) calculated by phase diagram mode of THERMOCALC. Schreinemakers [26] and Zen [27] rules are applied and the stability fields of six different parageneses are characterized.

6. 2. Muscovite+Biotite breakdown temperature

Reaction [r5] is used to place constraints on temperature of breakdown of muscovite and biotite in the Pichaghchi aureole of the Shahindezh area. The master equation in petrological thermodynamics and relative enthalpy, entropy, molar volumes and heat capacity data at standard condition are used for calculating the temperature of breakdown of muscovite and biotite. The position of the reaction on PT grid is shown in Fig. 8. P-T position of this curve is calculated by the means of conventional thermodynamic calculations using the following master equation.

$$0 = \Delta G^0_{(r)1,T} + (P-1)[\Delta V_S + \Delta(\alpha V)(T-298) - \Delta(\beta V)P/2] + RT\ln K$$

$$\Delta G^0_{(r)1,T} = \Delta H^0_{(r)1,298} + M - T(\Delta S^0_{(r)1,298} + N)$$

$$M = \int_{298}^{T} \Delta CP dT$$

$$N = \int_{298}^{T} \Delta CP/T dT$$

$$\Delta CP = \Delta a + \Delta bT + \Delta cT^{-2} + \Delta dT^{-0.5}$$

where ΔG is the Gibbs energy changes for the reaction, ΔV is the volume change, ΔH and ΔS refer to enthalpy (heat of reaction) and entropy changes, ΔC_P changes in the heat capacity and a, b, c and d are polynomial parameters. α is thermal expansion and β is pressure compressibility.

The equilibrium coefficient for reaction [r5] is calculated as below:

$$K = \frac{(aMg - Crd)^3 \times (aKfs)^8 \times (aH_2O)^8}{(aPhl)^2 \times (aQtz)^{15} \times (aMs)^6}$$

a shows the activity of mineral end-members which are calculated by AX program.

Since the ΔS of this reaction is positive, it is very likely for this reaction to occur in the thermal aureole. Also considering the larger ΔS than ΔV and regarding the Clausius-Clapeyron relation ($\frac{dP}{dT} = \frac{\Delta S}{\Delta V}$), this reaction should have a positive slope on the PT diagram. Using the pressure for the aureole discussed above and by constructing the reaction curve for [r5], the temperature of breakdown of muscovite + biotite is 650 ± 50°C. The temperature of breakdown for Mg end- members (phlogopite and Mg-

cordierite) is ~8 °C higher than breakdown temperature for Fe end- members (annite and Fe-cordierite). This temperature is in good agreement with temperature for crystallization of prismatic sillimanite in the aureole [e.g. 22].

According to some experimental data from Pattison [28], occurrence of this reaction at the pressure higher than 3.8 kbar, is impossible. Pattison [28] has suggested that at this pressure (which is close to calculated pressure for the SMC aureole) and with pure water content ($a_{H2O} = 1$), temperature of the reaction is ~ 660 °C. This is in excellent agreement with our finding (Fig. 8).

7. Partial Melting of metapelites

7. 1. Microstructure evidence for partial melting

The typical mineral assemblage in the migmatitic rocks at the NE-SMC is quartz + biotite + garnet + plagioclase ± cordierite ± K – feldspar + sillimanite (fibrous and/or prismatic) ± apatite ± ilmenite ± chlorite (alteration product). Garnet occurs as porphyroblasts which is commonly free of inclusions (Fig. 9a). In the rare cases garnet hosts irregular shaped quartz inclusions (Fig. 9b). Cordierite hosts fibrolite mats (Fig. 9c) and has replaced garnet rims in some samples (Fig. 9a). Commonly, it is also found as polygonal grains at the matrix with inclusions of fibrolite and ilmenite (Fig. 9c).

The partial melting related microstructures at the SMC aureole have been divided into 3 groups. At the first group garnet porphyroblasts have some irregular shaped quartz inclusions (Fig. 9b) or new crystals of quartz are formed around garnet (Fig.9d). Second group, in the sillimanite-rich rocks, consists of coarse, randomly oriented biotite and prismatic sillimanite (Fig. 9e), but in the biotite-rich hornfelses, sillimanite occurs only as trails of inclusions in cordierite or plagioclase (Fig. 9f). Prismatic sillimanite is commonly surrounded by a narrow channel of quartz (Fig. 9d). In third group cordierite is formed around garnet porphyroblasts and altered to pennite (Fig. 9a). Also cordierite in the matrix, without relationship with garnet, is observed which has fibrolite inclusions and is altered to pennite, too (Fig. 9c). In some samples, the partial replacement of cordierite with long flakes of biotite is happened.

Most of the above microstructures are well developed at the Proterozoic Namaqualand Metamorphic Complex, South Africa [9]; Shuswape metamorphic core complex, Canadian Cordillera [6] and Pointe Geologie migmatitic complex [3]. The microstructures explained above for the SMC aureole have the general features of partially molten metapelitic rocks.

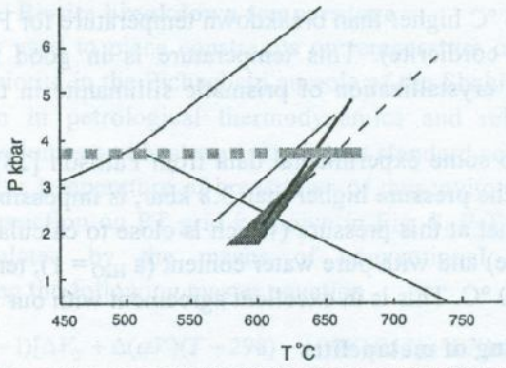

Fig. 8 Position of the reaction muscovite+biotite breakdown at the PT space. The heavy solid line shows the curve calculated in this study. The grey thick line is from experimental data of [28]. The thin solid line shows the position of the reaction on the petrogenetic grid suggested by [22]. The dashed heavy line is the reaction curve of muscovite breakdown on the [29] petrogenetic grid. There is a good agreement between the position of calculated curve in this study and Pattison's experimental based suggested curve.

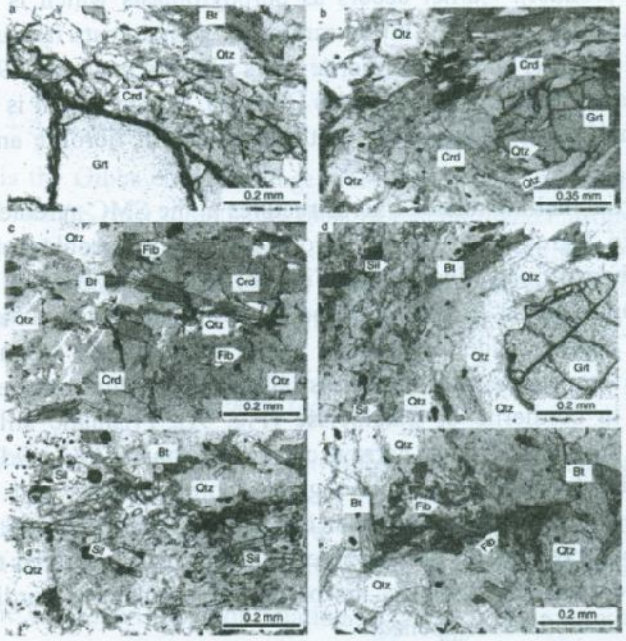

Fig. 9 Microphotographs of observed partial melting microstructures. a) Garnet porphyroblast without quartz inclusion, is surrounded by pennitizied cordierite. b) Garnet- quartz association. New cordierite (partial melting product) is crystallized at the garnet rim. c) Cordierite in the matrix without any relation with garnet. Fibrolite inclusions can be seen. d) A quartz channel between garnet porphyroblast and prismatic sillimanite. e) Biotite and prismatic sillimanite in the sillimanite-rich rock samples. f) Fibrolite has grown in the biotite-rich rocks as inclusion in the plagioclase and/or quartz.

7. 2. possible melting reactions

Anhydrous ferromagnesian porphyroblasts, which are the solid products of the dehydration melting of biotite, are formed in the partially melted rocks.

Bt + Sil + Pl + Qtz = Grt + Kfs + Melt [r7]

Bt + Sil + Pl + Qtz = Grt + Crd + Kfs + Melt [r8]

[30 - 33].

The reaction [r7] was responsible for generation of cordierite free assemblages and the reaction [r8] may explain the occurrence of cordierite around garnet porphyroblasts. It is possible that biotite-sillimanite associations are produced by reaction [r7] and [r8] operating at retrograde direction.

The followed reaction [34] could have been happened in the samples with cordierite:

Grt + Sil + Qtz = Crd [r9]

Decompression to some extent is necessary for the dehydration melting of metapelites to proceed by the following reaction:

Bt + Sil = Grt + Crd + melt [r10]

[35, 36].

No orthopyroxene was found at the SMC aureole, therefore, the orthopyroxene producing melting reaction may be used for estimating the upper limit of the temperature at the studied aureole (Fig. 10).

Bt + Pl + Qtz = Opx + Kfs + melt [r11]

7. 3. Interpretation

The processes that control the microstructure of migmatitic rocks during their prograde development and subsequent cooling, include both melt-present and subsolidus reactions. The latter may take place either in the absence or in the presence of aqueous fluid [9]. Ideally, microstructural criteria should be sought that allow these different processes to be distinguished [e.g. 9, 37]. Intergrowth textures reflect low diffusional mobility of major species, such as Al and Si [38 - 40]. Therefore, it is possible that, garnet-quartz association at the SMC, has been formed owing to low diffusional mobility of Al and Si. It has been argued that pre-existing garnet is a favorable location for the initiation of melting [30, 31]. Powell and Downes [41] inferred that all the garnets in leucosomes represented new garnet formed by the melting reaction. The irregular shape of quartz around garnet and intergrowth with it in the SMC aureole, suggests that the garnet

and quartz grew together [e.g. 9]. Coarse, clustered aggregates of sillimanite and biotite probably represent the products of direct back-reaction with melt. The estimated temperature for the SMC aureole is similar to that of the Pointe Geologie migmatitic complex obtained by Monnier [42]. The assemblage is biotite + cordierite + sillimanite + garnet in this area and the calculated temperature using THERMOCALC is 700 ± 50 °C at pressure ~ 4 kbar.

Also temperature at the sillimanite-cordierite zone of Shuswap metamorphic core in Canadian Cordillera have been calculated about 750 °C at the pressure less than 5 kbar [6]. Both of the Pointe Geologie and Shuswap metamorphic rocks are formed at the LP regional metamorphism. The SMC aureole is comparable to facies series 2 (2a) of Pattison [28]. High grade assemblages typically contain biotite + garnet + sillimanite + K – feldspar + cordierite (without staurolite) at this type of metamorphic terrains. Notable examples of this sub-facies series include the Cupsuptic aureole, Maine [43] and the Kiglapait aureole, Labrador [44]. According to the Pattison's category [45], the mineral assemblage of type 2a, is formed at the pressure about 3-4 kbar. We estimated this value of pressure for the SMC aureole using the thermodynamic data sets (Fig. 10).

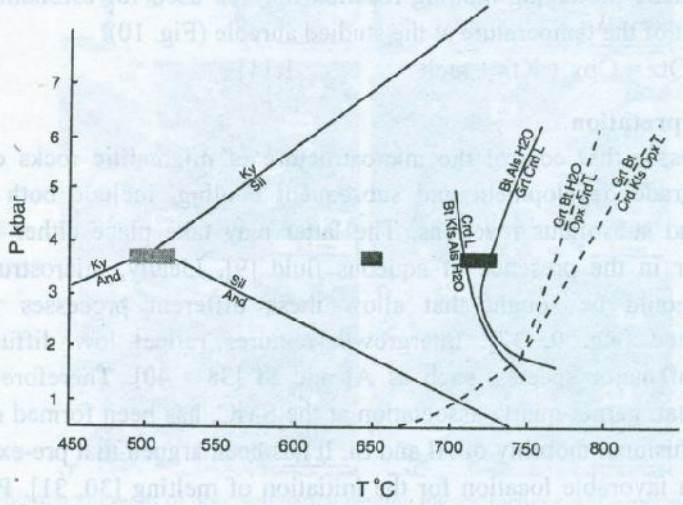

Fig. 10 The upper limit of temperature at the SMC partially melted rocks, using the petrogenetic grid after [29].The dark box shows the estimated T for partial melting in the studied rocks. The lighter box is the muscovite + biotite breakdown PT. The lightest box shows the PT, which the vast area of the SMC aureole has experienced.

8. Conclusions

The intrusion of the Pichaghchi batholith in the regional metamorphic rocks of the SMC has caused contact metamorphic overprint on these rocks. Pressure and temperature of contact metamorphism was estimated using microprobe analyses of the minerals and THERMOCALC. The obtained pressure is 3.8 ± 1 by multi-equilibria calculation.

The metapelites at vast part of SMC aureole have the assemblage quartz+ plagioclase + biotite + muscovite + chlorite + cordierite + andalusite ± fibrolite. This paragenesis is formed at temperature about 500 °C.

Temperature for breakdown of muscovite+biotite is calculated by conventional thermodynamic method, which is 650 ± 40 °C. This is in the stability field of sillimanite and can be confirmed by crystallization of prismatic sillimanite in the rocks close to the igneous contact. A few samples have experienced muscovite+biotite breakdown temperature, while the rest of area is metamorphosed at lower temperatures.

Only at the north-eastern part of the SMC, metapelites have experienced partial melting. Evidence for high-T metamorphism is partial replacement of old garnets by melting product cordierite, intergrowth of new garnet-quartz and prismatic sillimanite-biotite-quartz association. In the SMC rocks cordierite occurs around garnet, sillimanite and also in the matrix. Previous investigators have suggested that fine grained reaction products, coronas, partial replacement along the rim of grains and symplectitic textures are indicative of incomplete reactions. Since the SMC rocks lack orthopyroxene, the orthopyroxene formation dehydration melting reaction puts an upper limit on the temperature reached by the rocks. The present assemblage in the migmatitic rocks have remained stable during the retrograde history, meaning that very little water was introduced into the system.

Two main reasons can be considered for partial melting in the upper crust, (i) relatively isothermal decrease in pressure (e.g. decompression as a result of unroofing) and (ii) isobaric increase in temperature (e.g. heating during burial). Regarding the thermal influence of the Pichaghchi bathoilth, it seems that the concluded reaction for contact metamorphism and partial melting of pelites have taken place due to isobaric increase in temperature, more likely in a short time span. Distribution of metamorphic mineral parageneses and partially melted rocks on field (Fig. 1) shows that, at the north-eastern part of the SMC, granodioritic magma, has emplaced at the upper levels of the crust in comparison with central and western parts.

Acknowledgements

We would like to thank Prof. P. O'Brien from Potsdam University, Germany and Prof. D. Whitney from Minnesota University, USA for their help during this research.

Dr. Rhede and O. Appelt helped with microprobe analysis in GFZ, Potsdam, Germany.

References

[1] Powell R., Holland T.J.B., *"An internally consistent thermodynamic dataset with uncertainties and correlation: 3. Application to geobarometry, worked examples and computer program"*, J. Metamorph. Geol. 6 (1988) 173-204.

[2] Fyfe W.S., *"The granulite facies, partial melting and the Archaean crust"*, Philos. Trans. R. Soc. London, Ser. A, 273 (1973) 457–462.

[3] Pelletier A., Guiraudb M., Menot R.P., From partial melting to retrogression in the Pointe Geologie migmatitic complex: A history of heterogeneous distribution of fluids. Lithos 81: 153-166 (2005).

[4] White R.W., Powell R., Holland T.J.B., *"Calculation of partial melting in the system $Na_2O - CaO - K_2O - FeO - MgO - Al_2O_3 - SiO_2 - H_2O$ (NCKFMASH)"*, J. Metamorph. Geol. 19 (2001) 139– 154.

[5] Calvert, A.T., Gans, P.B., Amato, J.M., *"Diapiric ascent and cooling of a sillimanite gneiss dome revealed by 40Ar/39Ar thermochronology: the Kigluaik Mountains, Seward Peninsula,Alaska"*, In: Ring, U., Brandon, M.T., Lister, G.S., Willett, S.D. (Eds.), Exhumation Processes: Normal Faulting, Ductile Flow and Erosion. Geol. Soc. London (1999) 181–204.

[6] Norlander B.H., Whitney D.L., Teyssier C., Vanderhaeghe O., *"Partial melting and decompression of the Thor-Odin dome, Shuswap metamorphic core complex, Canadian Cordillera"*, Lithos 61 (2002) 103-125.

[7] Vanderhaeghe O., Teyssier C., *"Formation of the Shuswap metamorphic core complex during late-orogenic collapse of the Canadian Cordillera: role of ductile thinning and partial melting of the mid-to lower crust"*, Geodin. Acta 10 (1997) 41– 58.

[8] Vanderhaeghe O., Teyssier C., *"Crustal-scale rheological transitions during late-orogenic collapse"*, Tectonoph. 335 (2001) 211 – 228.

[9] Waters D.J., *"The significance of prograde and retrograde quartz-bearing intergrowth microstructures in partially melted granulite-facies rocks"*, Lithos 56 (2001) 97-110.

[10] Alavi-Naini, M. and Amidi, S.M., *"Geology of western parts of Takab Quadrangle"*, Geol. Surv. Iran. Note no 49 (1968) 98p.

[11] Haghipour A., *"Precambrian in Central Iran. Bull No 81 First Quarter"*, The Iranian Petroleum Institute, (1981).

[12] Khasragi K., Eghlimi M.H., Amini Azar B., Alavi-Naini R., *"Geological map of Sahindezh 1:100000"*, Geol. Surv. Iran. No.5363 (1994).

[13] Stocklin J., *"Structural history and tectonics of Iran (A review)"*, Am. Assoc. Petrol. Geol. Bull. pp. 1229 v 52:7 (1968).

[14] Berberian, M., King, C.P., *"Towards a paleogeography and Tectonic evolution of Iran"* Can. J. Ear. Sci. 18 (1981) 2.

[15] Haghipour A., *"Etude geologique de la region de Biabanak-Bafq (Iran Central); petrologie et tectonique du precambrien et de sa couverture"*, These, universite scientifique et medicale de Grenoble, France, (1974), 403p.

[16] Nabavi, M.H., "Geology of Iran", Geol. Surv. Iran 109p. (1975).

[17] Berberian, M., *"A brief geological description of north-central Iran. In materials for the study of seismotectonics of Iran: North-Central Iran"*, Geol. Surv. Iran. Rep. 29 (1974)127-138.
[18] Ramezani J., Tucker R.D., *"The Saghand region, central Iran: U-Pb geochronology, petrogenesis and implications for Gondwana tectonics"*, Am. J. Sci. 303 (2003) 622-665.
[19] Kholghi M.H., Vossoughi Abedini M., *"Origin, petrogenesis and radiometric age dating of Pichagchi batholite (North West Iran)"*, Geosci. Iran v. 11, no. 49-50 (2004) 78-89.
[20] Moazzen M., Homam S. M.,Ghaderi Zafreh H., *"A review of fibrolite problem and its formation condition in the thermal aureole of the Chahghand gabbro, Neyriz, southern Iran"*, Ir. J. Crys. Mineral. 1 (2006) 113-128.
[21] Kretz R., *"Symbole for rock-forming minerals"*, Am. Mineral. 68 (1983) 277-279.
[22] Spear F.S., Cheney J.T., *"A petrogenetic grid for pelitic schists in the system SiO_2-Al_2O_3-FeO-MgO-K_2O-H_2O"*, Contrib. Mineral. Petrol. 101 (1989) 149-164.
[23] Moazzen M., Modjarrad M., *"Contact metamorphism and crystal size distribution studies in the Shivar aureole, NW Iran"*, Geol. J. 40 (2005) 499-517.
[24] Dale J., Holland T.J.B., *"Geothermobarometry, P-T paths and metamorphic field gradients of high-P rocks from the Adula Nappe, Central Alps"*, J. Metamorph. Geol. 21 (2003) 813-829.
[25] Spear F.S., *"Metamorphic phase equilibria and Pressure-Temperature-Time Paths"*, Mineral Soc Am, (1993) 799p.
[26] Schreinemakers F.A.H., *"In-, mono-, and divariant equilibria"*, Koninkl Nederl Akad Wetenschap Amsterdam Proc. Reprinted as "Papers by F.A.H. Schreinmakers" Vol. 2 Penn. State Univ., Univ. Park, Pennsylvania, 1965 (1912-1925).
[27] Zen E-an., *"Construction of pressure-temperatures for multicomponent systems after the method of Schreinmakers: a geometric approach"*, U.S. Geol. Surv. Bull. 1225 (1966).
[28] Pattison D.R.M., *"P-T conditions and the influence of graphite on pelitic phase relations in the Ballachulish aureole, Scotland"*, J. Petrol. 30 (1989) 1219-1244.
[29] Wie C.J., Powell R., Clarke G.L., *"Calculated phase equilibria for low- and medium-pressure metapelites in the KFMASH and KMnFASH sestems"*, J. Metamorph. Geol. 22 (2004) 495-508.
[30] Waters D.J., Whales C.J., *"Dehydration melting and the granulite transition in metapelites from southern Namaqualand, S. Africa"*, Contrib. Mineral. Petrol. **88** (1984) 269–275.

[31] Waters D.J., *"Partial melting and the formation of granulite-facies assemblages in Namaqualand, South Africa"*, J. Metamorph. Geol. 6 (1988) 387–404.
[32] Vielzeuf D., Holloway J.R., *"Experimental determination of the fluid-absent melting reactions in the pelitic system"*, Contrib. Mineral. Petrol. 98 (1988) 257– 276.
[33] Stevens G., Clemens J.D., Droop G.T.R., *"Melt production during granulite-facies anatexis: experimental data from ''primitive'' metasedimentary protoliths"*, Contrib. Mineral. Petrol. 128 (1997) 352–370.
[34] Waters D.J., *"Metamorphic zonation and thermal history of pelitic gneisses from western Namaqualand, S. Africa"*, Trans. Geol. Soc. S. Afr. 89 (1986) 97–102.
[35] Carrington, D.P., Harley, S.L., *"Partial melting and phase relations in high-grade metapelites: an experimental petrogenetic grid in the KFMASH system"*, Contrib. Mineral. Petrol. 120 (1995) 270– 291.
[36] Spear F.S., Kohn M.J., Cheney J.T., *"P–T paths from anatectic pelites"*, Contrib. Mineral. Petrol. 134 (1999) 17–32.
[37] Vernon R.H., Collins W.J., *"Igneous microstructures in migmatites"*, Geol.16 (1988) 1126–1129.
[38] Cashman, K.V., *"Textural constraints on the kinetics of crystallization of igneous rocks"*, In: Nicholls, J. and Russell, J.K., Editors, 1990. Modern Methods of Igneous Petrology Mineral. Soc. Am., Rev. Mineral. 24 (1990) 259–314.
[39] Watson E.B., Baker D.R., *"Chemical diffusion in magmas: an overview of experimental results and geochemical applications"*, In: Perchuk, L.L. and Kushiro, I., Editors, 1991. Physical Chemistry of MagmasAdv. Phys. Geochem. vol. 9, Springer, New York, (1991) 120–151
[40] Barker, A.J., *"Introduction to Metamorphic Textures and Microstructures"*, 2nd edn. Stanley Thornes, Cheltenham. (1998).
[41] Powell R., Downes J., *"Garnet porphyroblast-bearing leucosomes in metapelites: mechanisms, phase diagrams, and an example from Broken Hill, Australia"*, In: Ashworth, J.R. and Brown, M., Editors, 1990. High-Temperature Metamorphism and Crustal AnatexisMineral. Soc. Ser. vol. 2, Unwin Hyman, London (1990) 105–123.
[42] Monnier O., *"Le socle prote´rozoRque de Terre Ade´lie (Antarctique Est)"*, Unpublished PhD thesis, University of Saint Etienne (1995) 321 pp.
[43] Bowers, J.R., Kerrick, D.M., Furlong, K.P., *"Conduction model for the thermal evolution of the Cupsuptic aureole, Maine"*, Am. J. Sci. 290 (1990) 644-665.
[44] Berg, J.H., Docka, J.A., *"Geothermometry in the Kiglapait contact aureole, Labrador"*, Am J Sci 283 (1983) 414-434.
[45] Pattison D.R.M., *"Stability of andalusite and sillimanite and the Al_2SiO_5 triple point: Constraints from the Ballachulish aureole, Scottland"*, J. Geol. 100 (1992) 423-446.